Proceedings Title IAU Symposium
Proceedings IAU Symposium No. 231, 2005
A.C. Editor, B.D. Editor & C.E. Editor, eds.

doi:10.1017/S1743921306007101

Dissociative Recombination of $CD_3OD_2^+$

W. D. Geppert[1], F. Hellberg[1], F. Österdahl[2], J. Semaniak[3], T. J. Millar[4], H. Roberts[4], R. D. Thomas[1], M. Hamberg[1], M. af Ugglas[1], A. Ehlerding[1], V. Zhaunerchyk[1], M. Kaminska[3], and M. Larsson[1]

[1]Molecular Physics Division, Department of Physics, Stockholm University, AlbaNova, SE 10691, Stockholm, Sweden, e-mail: wgeppert@physto.se

[2]Institute of Physics, Royal Institute of Technology, AlbaNova, SE 10691, Stockholm, Sweden

[3]Świętokrzyska Akademy, ul. Świętokrzyska 15, Pl-245406 Kielce, Poland

[4]University of Manchester, Manchester M13 9PL, United Kingdom

Abstract. The branching ratios of the different reaction pathways and the overall rate of the dissociative recombination of $CD_3OD_2^+$ were measured at the CRYRING storage ring located at the Manne Siegbahn Laboratory in Stockholm, Sweden. A preliminary analysis of the data yielded that formation of methanol accounts for only 6 ± 2 % of the total reaction rate. Largely, dissociative recombination of $CD_3OD_2^+$ involves fragmentation of the C–O bond, the major process being the three-body break-up forming CD_3, OD and D (branching ratio 0.59). A non-negligible formation of interstellar methanol by the previously proposed mechanism is therefore very unlikely.

Keywords. ISM: molecules — methods: laboratory — molecular processes

1. Introduction

Methanol is one of the most important and interesting interstellar compounds. It is well known that masers of methanol are associated with the early stages of formation of high-mass stars. Observations of methanol densities are also used to determine the temperature and density of a molecular cloud simultaneously (Leurini *et al.* 2004). Furthermore, the compound can be used as an evolutionary indicator during the embedded phase of massive star formation (van der Tak, van Dishoeck & Caselli 2000).

The formation of interstellar methanol has puzzled scientists for a long time. Since grain-surface processes were not thought to be able to produce the observed methanol densities (Allen & Robinson 1977), gas-phase reactions have been regarded as the major source of this molecule in space. Up to now, it had been widely accepted that the first step of interstellar methanol formation is a radiative association of CH_3^+ and H_2O followed by dissociative recombination (DR) leading to CH_3OH and H:

$$CH_3^+ + H_2O \rightarrow CH_3OH_2^+, \tag{1.1}$$

$$CH_3OH_2^+ + e^- \rightarrow CH_3OH + H. \tag{1.2}$$

Generally, radiative association reactions tend to have very low thermal rates. However, in the case of formation of a large stable molecular ion, the radiative lifetime of the intermediately formed excited complex can exceed its dissociative lifetime and, consequently, a stable ion can be formed. This has, e. g. been observed in the radiative association of C_3H^+ and H_2 (Sorgenfrei & Gerlich 1994). For larger systems it has then been assumed

that rates of radiative associations are collisional and can exceed 10^{-9} cm^3 s^{-1} (Herbst & Dunbar 1991). To explain the observed interstellar abundances of methanol it has been postulated that the rate for radiative association should lie in the range between 8×10^{-12} cm^3 s^{-1} and 8×10^{-8} cm^3 s^{-1}(Gottlieb *et al.* 1979). Indeed, a radiative association reaction of $\sim 2 \times 10^{-10}$ cm^3 s^{-1} at 300 K has been obtained in a SIFT experiment (Smith & Adams 1977).

But recently, it has been shown in an ion trap experiments that the rate of the radiative recombination of CH_3^+ and H_2O amounts to maximally 2×10^{-12} cm^3 s^{-1} and therefore is at least a factor of 10 too low to explain the interstellar abundances of methanol if one applies the common astrochemical models used (Luca, Voulot & Gerlich 2002; Herbst 1985). However, since CH_3^+ has never been observed, its abundances in interstellar clouds and other astronomical environments might differ considerably from model predictions. Therefore a substantial contribution of the proposed mechanism to the formation of interstellar methanol cannot yet be ruled out. Nevertheless, this only holds under the assumption that the dissociative recombination (DR) of $CH_3OH_2^+$ mostly or exclusively leads to methanol. Exact knowledge of the branching ratio of $CH_3OH_2^+$ is therefore necessary to be able to finally disregard the gas-phase formation mechanism according to equations (1.1) and (1.2).

This contribution presents the determination of the rate and the branching ratios of the DR of $CD_3OD_2^+$ at relative kinetic energies encountered in dark interstellar clouds.

2. Experimental

The DR experiments have been performed at the heavy-ion storage ring CRYRING at the Manne Siegbahn Laboratory, Stockholm University. Since the experimental procedure has been described in detail elsewhere (Neau *et al.* 2000), it is summarized only briefly here. For technical reasons related to the data analysis (better mass resolution on the surface barrier detector), $CD_3OD_2^+$ was used in the present experiment. The $CD_3OD_2^+$ ions were produced in a discharge ion source from a mixture of methanol vapor and deuterium (in excess). After extraction of the ions from the source at 40 keV energy, they were mass selected, injected into the ring and accelerated to 2.53 MeV translational energy. The stored ion beam was merged with a mono-energetic electron beam in an electron cooler, the length of the interaction region being 0.85 m. During the first 3 s after acceleration, the electron and ion beams were kept at the same average velocity to allow heat transfer from the ion to the electron beam in order to reduce the translational temperature of the ions which results in an increase of their phase-space density. Furthermore, such a storage time enables radiative vibrational cooling of the ions, which might partially have been formed in a rovibrationally excited state.

Neutral products generated by DR reactions in the electron cooler leave the ring tangentially and were detected by an energy-sensitive silicon surface barrier detector (SBD) with a diameter of 17 mm mounted at a distance of 4.30 m from the center of the interaction region. A background signal due to neutral products emerging from collisions of the ions with residual gas was also present; this was measured with the relative translational energy between the ions and electrons tuned to 1 eV, where the DR cross section is very low and the measured neutral fragments are therefore almost exclusively produced by rest gas collisions. This background was subsequently subtracted from the total SBD signal.

https://doi.org/10.1017/S1743921306007101 Published online by Cambridge University Press

3. Results

3.1. *Absolute Cross Section and Thermal Reaction Rate*

During cross section measurements, the relative translational energy between the ions and the electrons was continuously varied between 1 and 0 eV. This was achieved by changing the cathode voltage of the electron cooler over 1 s from a high value corresponding to a centre-of-mass energy of 1 eV, the electrons being faster than the ions, down to a low value also corresponding to 1 eV but where the electrons were slower than the ions. Thus, a voltage corresponding to a centre-of-mass energy of 0 eV is reached during the scan. Before the measurement was started, 3 s of cooling, with the electrons tuned to 0 eV collision energy, was carried out. The signal from the SBD was monitored by a single-channel analyser, selecting signals arising from all fragments reaching the detector simultaneously and thereafter recorded by a multichannel scaler, yielding the number of counts vs. storage time and, therefore, at a given relative translational collision energy.

The experimental DR rate coefficient in the electron cooler is expressed by the formula:

$$\langle v_{cm}\sigma\rangle = \left(\frac{dN}{dt}\right) = \frac{v_i v_e e^2 r_e^2 \pi}{I_e I_i l} \tag{3.1}$$

where dN/dt is the number of counts per unit time, v_i and v_e are the electron and ion velocities, respectively, r_e is the radius of the electron beam, l the length of the interaction region, and I_e and I_i are the electron and ion current, respectively.

Simultaneously with the measurement of the dissociative recombination count rate, the ion current was monitored using a Bergoz beam charge monitor, with continuous averaging, and an AC integrating current transformer combination with a neutral particle detector installed at the end of one of the straight sections of the ring (Paal *et al.* 2004). Continuous measurement of neutral products due to the ion-rest gas collisions also allowed the decay of the ion beam to be monitored during each injection. The following corrections to the measured data had to be performed. Firstly, the voltage of the electron cooler cathode (and therefore v_e) had to be corrected for space charge effects. Secondly, the measured rate coefficient $\langle v_{cm}\sigma\rangle$ had to be adjusted because of the toroidal effect (Lampert *et al.* 1996). The toroidal effect stems from the zones at both ends of the interaction region where the electron beam is bent into or out of the ion beam. In these regions, the transversal electron velocity is higher than in the merged interaction region leading to larger collision energies. Thirdly, the electron beam has (in contrast to the ion beam) a non-neglectible energy spread, and the measured reaction rate $\langle \sigma v_{cm}\rangle$ has to be deconvoluted according to the formula:

$$\langle v_{cm}\sigma\rangle = \int_{-\infty}^{\infty} v_e f(v_e)\sigma(v_e) d^3 v_e \tag{3.2}$$

where $f(v_e)$ is the velocity distribution. From the resulting rate constants, the (comparatively) very small contribution to the data due to charge transfer processes with the rest gas had to be subtracted. Since the cross section of the DR is very low at 1 eV collision energy, and the rest gas collisions are independent of the electron velocity, the signals measured at this energy were assumed to be due solely to charge transfer. The cross-sectional data are best fitted by the expression $\sigma = 9.6 \pm 1.9 \times 10^{-15}\ E^{-0.96\pm0.02}\ \mathrm{cm}^2$. The thermal reaction rate constant can be deduced from the cross sections by applying the formula

$$kT = \frac{8\pi m_e}{(2\pi m_e kT)^{3/2}} \int_0^{\infty} E\sigma(E) e^{-\frac{E}{kT}} dE \tag{3.3}$$

https://doi.org/10.1017/S1743921306007101 Published online by Cambridge University Press

where m_e is the mass of the electron. The temperature dependence of the rate coefficient can then be fitted to the expression $9.1 \pm 1.8 \times 10^{-7}(T/300)^{-0.63}$ cm^3 s^{-1}.

3.2. *Branching Ratios*

In the DR of $CD_3OD_2^+$ the following exoergic reaction channels exist:

$$CD_3OD_2^+ + e^- \rightarrow CD_3 + D_2O \qquad \Delta H = -6.87eV \tag{3.4a}$$
$$CD_3OD_2^+ + e^- \rightarrow CD_3 + OD + D \qquad \Delta H = -1.70eV \tag{3.4b}$$
$$CD_3OD_2^+ + e^- \rightarrow CD_2 + D + D_2O \qquad \Delta H = -2.12eV \tag{3.4c}$$
$$CD_3OD_2^+ + e^- \rightarrow CD + D_2 + D_2O \qquad \Delta H = -2.32eV \tag{3.4d}$$
$$CD_3OD_2^+ + e^- \rightarrow CD_3OD + D \qquad \Delta H = -5.70eV \tag{3.4e}$$
$$CD_3OD_2^+ + e^- \rightarrow CD_3O + D_2 \qquad \Delta H = -5.70eV \tag{3.4f}$$
$$CD_3OD_2^+ + e^- \rightarrow CD_3O + 2D \qquad \Delta H = -1.18eV \tag{3.4g}$$
$$CD_3OD_2^+ + e^- \rightarrow CD_2O + D + D_2 \qquad \Delta H = -4.81eV \tag{3.4h}$$
$$CD_3OD_2^+ + e^- \rightarrow CD_2O + 3D \qquad \Delta H = -0.29eV \tag{3.4i}$$
$$CD_3OD_2^+ + e^- \rightarrow CD_4 + O + D \qquad \Delta H = -1.81eV \tag{3.4j}$$
$$CD_3OD_2^+ + e^- \rightarrow CD_4 + OD \qquad \Delta H = -6.24eV \tag{3.4k}$$
$$CD_3OD_2^+ + e^- \rightarrow CD_2 + OD + D_2 \qquad \Delta H = -1.47eV \tag{3.4l}$$
$$CD_3OD_2^+ + e^- \rightarrow CD_3 + O + D_2 \qquad \Delta H = -1.78eV \tag{3.4m}$$
$$CD_3OD_2^+ + e^- \rightarrow CDO + 2D_2 \qquad \Delta H = -5.42eV \tag{3.4n}$$
$$CD_3OD_2^+ + e^- \rightarrow CDO + D_2 + 2D \qquad \Delta H = -0.94eV \tag{3.4o}$$
$$CD_3OD_2^+ + e^- \rightarrow CO + 2D_2 + D \qquad \Delta H = -4.76eV \tag{3.4p}$$
$$CD_3OD_2^+ + e^- \rightarrow CO + D_2 + 3D \qquad \Delta H = -0.28eV \tag{3.4q}$$

With the use of a storage ring, branching ratios can be determined even for DR reactions possessing a multitude of product pathways such as the case for $CD_3OD_2^+$. The fragments produced by a DR event reach the detector within a very short time interval compared with the integration time of the detection system. Owing to that fact, the pulse height of the SBD signal is proportional to the kinetic energy carried by the products of the reaction and therefore their total mass. To measure the branching ratios of the DR channels, a metal grid with a transmission $T = 0.297 \pm 0.015$ is inserted in front of the detector (Neau *et al.* 2000). Particles stopped by the grid do not reach the detector, and DR events where one of the fragments has been stopped result in a signal whose amplitude is proportional to the kinetic energy of the detected fragment. The registered DR spectrum therefore splits into a series of peaks with different energies, the intensities of which can be expressed in terms of the branching ratios and the probabilities of the particles passing the grid. For example, the intensity of the CD_3 peak emerging from reaction (3.4*a*) is proportional to $T(1-T)\alpha$, with α being the branching ratio of reaction (3.4*a*) and $T(1-T)$ the probability of only the CD_3 fragment passing the grid, respectively. The energy spectrum of the $CD_3OD_2^+$ DR reaction is shown in Figure 1. The different signal peaks are reasonably resolved and were therefore could be fitted to double gaussian functions to allow the peaks to be slightly asymmetric. As can easily be seen in Figure 1, the final fitting curve is in very good agreement with the data.

https://doi.org/10.1017/S1743921306007101 Published online by Cambridge University Press

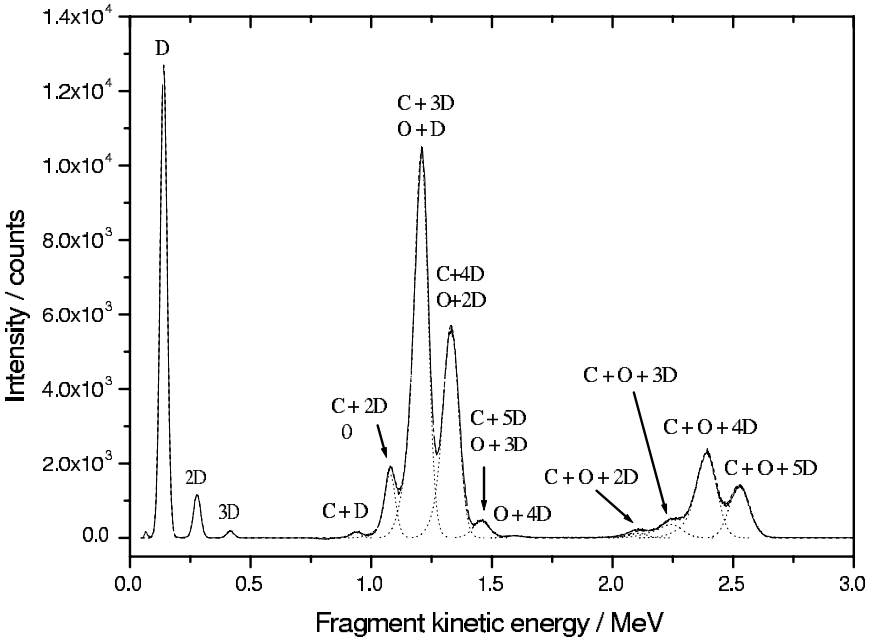

Figure 1. Fragment energy spectrum of protonated methanol with the grid in place. The solid line shows the data, the dotted lines the double-Gaussian fitting curves, and the dashed line the total fit.

Concerning the evaluation of the data, two problems arise. Firstly, some of the different channels produce products with the same mass distribution, leading to an identical signal distribution in the fragment energy spectrum spectrum. This holds for channels (3.4a) and (3.4k), (3.4c) and (3.4j) as well as (3.4l) and (3.4m; therefore, there exist three pairs of indistinguishable channels. However, since formation of CD_4 would involve a considerable rearrangement of the intermediately formed neutral, it can be argued that channels (3.4j) and (3.4k) are unlikely to play a major role. We will see later that the branching ratio of channel (3.4l) and (3.4m) is 0. Furthermore, since there is no signal corresponding to the mass of CO and DCO, channels (3.4n), (3.4o), (3.4p) and (3.4q) can be disregarded.

Secondly, owing to the high-energy release of reactions (3.4e) and (3.4f) and the comparatively low mass of the D and D_2 fragments, some of the deuterium atoms and molecules produced by these pathways might receive a large transversal velocity relative to the propagation direction, and therefore miss the detector. In the case of reaction (3.4e) this reduces the contribution of reaction (3.4e) to the C + 5H + O energy (mass) peak to $T^2(1-L)\varepsilon$, where L is the D-atom loss factor and ε denotes the branching ratio of channel (3.4e). Conversely, the C + 4H + O energy channel is augmented to $T(1-T)(1-L)\varepsilon + T\varepsilon L$. If one assumes that the whole reaction enthalpy is converted to kinetic energy, one would obtain a D loss of 67% for reaction (3.4e) and a D_2 loss of 13% for reaction (3.4f). Using the transmission probabilities together with the necessary corrections, a matrix is formulated for the relative intensities of the different energy (mass) peaks.To evaluate the loss of the deuterium atoms, an energy spectrum, shown in Figure 2, was measured with the grid removed. Since for this case $T = 1$ and the sum of all branching ratios amounts to 1, it can easily be worked out that the ratio between the

https://doi.org/10.1017/S1743921306007101 Published online by Cambridge University Press

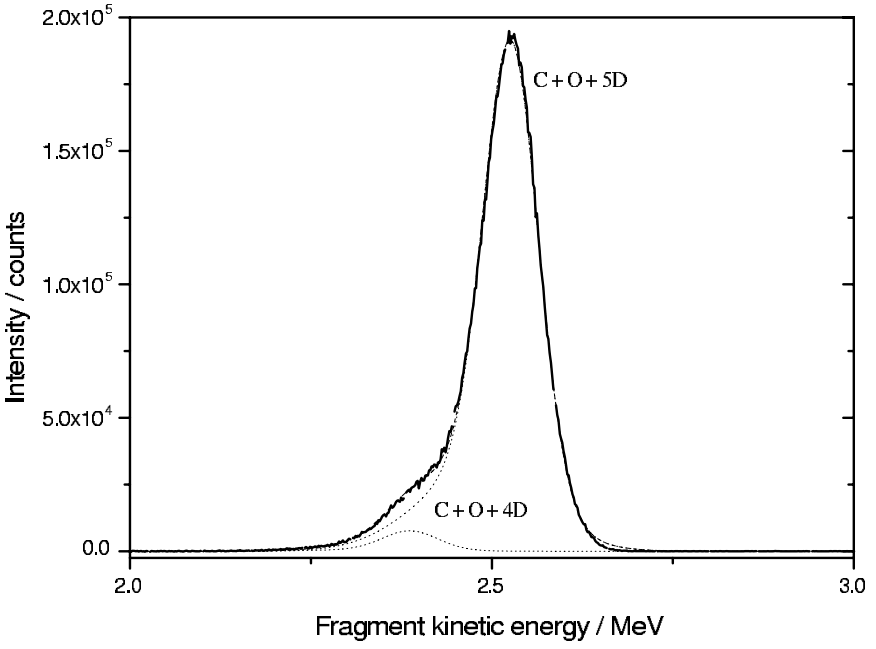

Figure 2. Fragment energy spectrum of protonated methanol with the grid removed. The solid line shows the data, the dotted lines the double Gaussian fitting curves and the dashed line the total fit.

Table 1. Branching ratios of the dissociative recombination of $CD_3OD_2^+$.

Reaction channel	Products	Branching ratio
a $(+k)$	CD_3 + D_2O	0.11
b	CD_3 + OD + D	0.59
$c(+j)$	CD_2 + D + D_2O	0.17
d	CD + D_2 + D_2O	0.01
e	CD_3OD + D	0.06
f	CD_3O + D_2	0.05
g	CD_3O + 2D	0.00
h	CD_2O + D + D_2	0.02

intensities of the C + O + 4D peak ($I_{(C+O+4D)}$) and the C + O + 5D ($I_{(C+O+5D)}$) peak will be:

$$\frac{I_{(C+O+4D)}}{I_{(C+O+5D)}} = \frac{\varepsilon L}{1-\varepsilon L} \tag{3.5}$$

No contribution of the C+O+3D mass was detected, therefore $L\zeta$ equals 0. By iteratively solving the matrix with a certain loss and calculating L according to (3.5), the loss of D-atoms, L, was determined to be 0.56 and the branching ratios listed in Table 1 were obtained.

3.3. *Model Calculations*

The new data on the rate and the branching ratios of dissociative recombination were used as an input for a model calculation of a dark cloud resembling TMC-1 using the

https://doi.org/10.1017/S1743921306007101 Published online by Cambridge University Press

UMIST code (Markwick, Millar & Charnley 2000). Using the previous data, the model predicted a peak abundance relative to H_2 of 1×10^{-9}, which is in good agreement with the observations of Friberg *et al.*, which yielded a methanol abundance in the low digits of 10^{-9} for TMC-1. (Friberg *et al.* 1988). With the present rate and branching rations of the dissociative recombination of protonated methanol, the peak abundance is lowered to 8×10^{-11}, while the one for steady-state sinks from 3×10^{-10} to 2×10^{-11}. If also the new rate for the radiative association of CH_3^+ and H_2O is included, the peak abundance is further lowered to 7×10^{-13} and the steady state to 1×10^{-13}, which is clearly below the observed values in dark clouds and probably below the detection limits for existing telescopes.

4. Discussion

The most striking feature of the DR of $CD_3OD_2^+$ is the low branching ratio of the "expected" channel leading to CD_3OD and D and the predominance of pathways involving 3-body break-ups. This is contrary to the theory formulated by Bates (1986), according to which the channel involving the least rearrangement of orbitals should be favored. However, recent research on DR branching ratios showed that these processes very often do not follow this prediction and three-body break-ups are actually quite common (see e.g. Larsson & Thomas 2001; McCall *et al.* 2004). It is interesting to compare the present findings to the ones obtained for the somewhat related H_3O^+ and D_3O^+ ions. With these species, pathways leading to three products also dominate with a total branching ratio of 0.61 and 0.60, respectively and the channels leading to H_2O and D_2O (branching ratios 0.25) are of minor importance (Jensen *et al.* 2000). These findings are similar to our results for $CD_3OD_2^+$, where the branching ratios of all three-body pathways add up to 0.78.

From the model calculations it ultimately becomes clear that the proposed gas-phase process (radiative association of $CH_3{}^+$ and H_2O with subsequent DR) cannot account for the production of interstellar methanol. Therefore, repetitive H-atom addition to CO on interstellar CO-containing ices seems the only plausible mechanism for methanol formation in the interstellar medium. This is corroborated by the fact that recent observations found a correlation between the abundances of methanol and CO in star-forming regions (Bisschop, Jørgensen & van Dishoeck 2005). Also, comparison of modelled and and observed deuterium fractionation in methanol points to a grain-surface process (Parise *et al.* 2004).

However, two problems are associated with this assumption: (a) Is the addition of H on solid CO efficient enough in forming methanol at the low temperatures that are encountered in dark interstellar clouds? (b) Can methanol be released from grain surfaces in sufficient quantities to explain the observed abundances not only in hot cores but also in dark clouds?

Very recently, it has been established experimentally, that the formation of methanol on pure CO and mixed CO/H_2O ices proceeds efficiently at 10 K (Watanabe *et al.* 2004) and the obtained yields of methanol are consistent with observations. Hydrogenation of the precursor methoxy or hydroxymethyl radicals is highly exoergic (–435.1 and –393.1 kJ mol^{-1}, respectively (Lias *et al.* 1988)) and might lead to methanol in a highly excited states and the resulting methanol molecule might use a part of this energy to recoil from the surface and end up in the gas phase. The question to what extent this is possible still lacks a definitive answer.

https://doi.org/10.1017/S1743921306007101 Published online by Cambridge University Press

Acknowledgements

Financial support from the Swedish Space Board and the Swedish Science Council is gratefully acknowledged.

References

Allen, M. & Robinson, G.W. 1977, *Ap. J.* 212, 396
Bates D.R. 1986, *Ap. J. Lett.* 306, 45
Bisschop, S.E., Jørgensen, J.K., & van Dishoeck, E.F. 2005, *IAU Symposium No. 231*, poster
Friberg, P., Madden, S.C., Hjalmarson, Å., & Irvine, W.M. 1988, *A&A* 195, 281
Gottlieb, C.A., Ball, J.A., Gottlieb, E.W., & Dickinson, D.F. 1979, *Ap. J.* 227, 422
Herbst, E. 1985, *Ap. J.* 291, 226
Herbst, E. & Dunbar, R.C. 1991, *MNRAS* 253, 341
Jensen, M.J., Bilodeau, R.C., Safvan, C.P., Seiersen, K., Andersen, L.H., Pedersen, H.B., & Heber, O. 2000, *Ap. J.* 543, 764
Lampert, A., Wolf, A., Habs, D., Kenntner, J., Kilgus, G., Schwalm, D., Pindzola, M., & Badnell, N. 1996, *Phys. Rev. A.* 53, 1413
Larsson, M. & Thomas, R.D. 2001, *Phys. Chem. Chem. Phys.* 3, 4471
Lias, S.G., Bartmess, J.E., Liebman, J.E., Holmes, J.L., Levin, R.D., & Mallard, W.G. 1988, *J. Phys. Chem. Ref. Data* 17
Leurini, S., Schilke, P., Menten, K.M., Flower, D.R., Pottage, J.T., & Xu, L.-H. 1985, *A&A* 422, 573
Luca, A., Voulot, D., & Gerlich, D. 2002, *WDS02 Proceedings of Contributed Papers, PART II* 294
Markwick, A., Millar, T.J., & Charnley, S.B. 2000, *Ap. J.* 535, 256
McCall, B.J., Huneycutt, A.J., Saykally, R.J., Djuric, N., Dunn, G.H., Semaniak, J., Novotny, O., Al-Khalili, A., Ehlerding, A., Hellberg, F., Kalhori, S., Neau, A., Thomas, R.D., Paal, A., Österdahl, F., & Larsson, M. 2004, *Phys. Rev. A* 70, 052716
Neau, A., Al-Khalili, A., Rosén, S., Le Padellec, A., Derkatch, A.M., Shi, W., Vikor, L., Larsson, M., Nagard, M.B., Andersson, K., Danared, H., & af Ugglas, M. 2000, *J. Chem. Phys.* 113, 762
Paal, A., Simonsson, A., Källberg, A., Dietrich, & Mohos, I. 2004, in *Proceedings of EPAC 2004 Lucerne*, 2743
Parise, B., Castets, A., Herbst, E., Caux, E., Ceccarelli, C., Mukhopadhyay, I., & Tielens, A.G.G.M 2004, *A&A* 416, 159
Smith, D. & Adams, N.G. 1977, *Ap. J.* 217, 741
Sorgenfrei, A. & Gerlich, D. 1994, in *Physical Chemistry of Molecules and Grains in Space*, ed. I. Nenner (AIP Press, New York), 505
van der Tak, F.F.S., van Dishoeck, E.F., & Caselli, P. 2000, *A&A* 361, 327
Watanabe, N., Nagaoka, A., Shiraki, T., & Kouchi, A. 2004, *Ap. J.* 616, 638